Author/s:
Medina-Cetina, Z;Yousefpour, N;Briaud, JL

Title:
Probabilistic evaluation of unknown foundations for scour susceptible bridges

Date:
2020-10-01

Citation:
Medina-Cetina, Z., Yousefpour, N. & Briaud, J. L. (2020). Probabilistic evaluation of unknown foundations for scour susceptible bridges. Journal of Bridge Engineering, 25 (10), https://doi.org/10.1061/(ASCE)BE.1943-5592.0001569.

Persistent Link:
https://hdl.handle.net/11343/274871

BE4257

Probabilistic Evaluation of Unknown Foundations for Scour-Susceptible Bridges

1. Zenon Medina-Cetina, PhD; Associate Professor, Texas A&M University, College Station, Texas 77840; zmedina@civil.tamu.edu.

2. **Negin Yousefpour**, PhD, PE; Research Assistant, Texas A&M University, College Station, Texas 77840 – **Corresponding Author**; negin.yousefpour@arup.com; Current affiliation: Senior Engineer, Arup, New York, NY 10005

3. Jean-Louis Briaud, PhD, PE; Distinguished Professor, Texas A&M University, College Station, Texas 77840; jbriaud@civil.tamu.edu.

ABSTRACT

As of 2005, approximately 60,000 bridges throughout the United States were identified as having unknown foundations. The Federal Highway Administration (FHWA) has required Departments of Transportation (DOTs) across the states to evaluate the safety of these bridges, particularly against scour failure, and reclassify them in the National Bridge Inventory (NBI). A probabilistic methodology was developed in this study to predict the type, embedment depth, and dimensions of unknown bridge foundations and to rigorously quantify the uncertainty of the predictions. This methodology uses Artificial Neural Networks (ANNs) to predict the expected values of bearing capacity (BC) using available information on bridge loading, soil strength, location, and year built, among other parameters. The unknown foundation characteristics are then evaluated using the Bayesian inference method and Markov-chain Monte-Carlo simulations, based on the predicted BC by the ANN models. The proposed method was validated based on a case study and proved successful in providing reasonable estimates on minimum foundation embedment depth for scour failure risk assessments. Transportation management authorities can adopt this method to reclassify bridges with unknown foundations and to implement risk-based decision-making approaches for bridge management.

Keywords: Bayesian Inference, Markov-chain Monte-Carlo, Unknown Foundations, Bridge Scour, Inverse Problems, Artificial Neural Networks

INTRODUCTION

Following the Federal Highway Administration (FHWA) requirement to inspect and monitor all bridges across the United States, a significant number of bridges were found to have no information available relating to their foundations (FHWA 2011). As of 2005, approximately 60,000 Unknown Foundation Bridges (UFBs) have been identified. Many of these bridges are over streams and rivers, hence susceptible to scour failure. Most of these bridges are classified as "off-system" bridges built by counties and local agencies, and later inherited by a Departments of Transportation (DOT).

Scour failure accounts for 60% of bridge failures, being the number one cause of bridge collapse in the US. For UFBs, evaluating scour failure probability is impossible due to lack of foundation design records. Therefore, evaluating the scour failure risk for these bridges has been a critical issue for DOTs across the US. The current condition of a bridge regarding its vulnerability to scour is recorded in the National Bridge Inventory (NBI) by Item 113, Scour-Critical Bridge Index. This item uses a single digit index which varies between 0 and 9, with 0 being the most scour-critical and 9 the least scour-critical. A "U" index is assigned to bridges with unknown foundation, indicating the risk due to scour is unknown (Weseman 1995). In the past two decades, DOTs have examined various methods to reclassify UFBs, however no breakthrough solution have been established yet.

Previous efforts on the determination of unknown foundations were mainly methods based on Non-Destructive Testing (NDT), including structural response measurements (Maser et al. 1998), acoustic methods such as Echo Response, Ultra-Seismic, Bending Wave, Borehole Sonic (Olson et al. 1998), and Parallel Seismic (Mercado and O'Neill 2003), as well as Field Modal Vibration (Olson 2005), Induction (Robinson and Webster 2008), Electrical Resistivity Imaging (ERI), and Induced Polarization methods (IP) (Briaud et al. 2011). Moreover, few studies have been performed using data mining and artificial intelligence (AI) technics, such as Artificial Neural Networks (ANNs) to infer scour depth at bridge piers (Bateni et al.

2007; Lee et al. 2007; Zounemat-Kermani et al. 2009; Kaya 2010), and to infer pile embedment depth (Mclemore et al. 2010; Sayed et al. 2011). Rix et al. (1995) explored the use of ANNs to interpret the results of NDTs for determination of UFBs. A risk-based method was also developed by Stein and Sedmera (2006) and Mclemore et al. (2010) using ANNs for management of UFBs susceptible to scour.

A deterministic evidence-based approach using ANNs has been already introduced by the authors to predict the type and the embedment depth of unknown foundations (Yousefpour et al. 2014). The proposed method predicts foundation characteristics based on available evidence of a bridge, including superstructure characteristics, loading, year built, and location. However, the ANN models naturally carry some uncertainties inherited from their input parameters, as well as the model parameters, such as weights and biases that are estimated through a deterministic optimization process. These uncertainties need to be quantified and addressed based on a rigorous statistical approach.

In all the above studies, ANNs proved to be a powerful predictive tool for evaluating scour and foundation embedment depth, based on directly or indirectly related parameters. ANNs specifically showed superior to conventional regression (linear and nonlinear) methods in highly-dimensional, nonlinear problems such as scour and foundation embedment depth prediction, by implicitly learning the inherent relationship between input parameters and the target parameter in the training database. Also, in comparison to NDT methods, solutions based on AI and data-driven methods, such as ANNs, are significantly faster and more cost-effective. On the other hand, ANNs are "data-hungry" and require large amount of data for training, which can be challenging to access and collect. Also, the ANN methods mentioned above provide deterministic solutions by single predictions, without proper assessments of uncertainty, as explained earlier.

In this study, a probabilistic approach is proposed that provides measures of uncertainty in the unknown foundation evaluation process. This methodology applies ANNs to predict the expected bearing capacity (BC) of an unknown foundation, which is then used to update the existing foundation information, using Bayesian inference. BC is predicted based on bridge loading, soil parameters (if known), location, and year of built. Likely foundation characteristics are estimated by generating probability distributions for the type, embedment depth, and dimensions. In addition, soil strength parameters can be estimated, in case soil boring data is missing. This study shows the benefits of Bayesian updating and the significance of data collection in predicting unknown foundations. The proposed methodology was implemented and cross-validated using data collected from bridges in the Bryan District of TxDOT, primarily built from 1960 to 2000. Similar to its existing counterparts, the proposed method has been developed with a specific application scope, and inevitably includes limiting assumptions that should be taken into account when evaluating a UFB, as elaborated later on in the paper.

DATA COLLECTION

There are approximately 1,700 bridges in the Bryan District of TxDOT, 1,100 of which are built over rivers and streams and are subjected to potential failure due to scour. The data available for superstructure, substructure, and soil conditions was collected for approximately 40% of the on-system bridges built over rivers in the Bryan District (about 185). This data was extracted for interior piers of bridges from the NBI (Weseman 1995), and from local bridge inspection inventories and construction plans. The selected bridges were sampled from four sub-populations of bridges with distinct foundation types, including: Drilled Shafts (*DrSh*), Concrete Piling (*Conc*), Steel Piling (*Steel*), and Spread Footing (*Spread*). Figure 1 presents the location of these bridges in the Bryan District of TxDOT, showing the Scour-Critical Bridge Index and year built. Table 1 presents a list of the key parameters included in the accumulated database with the corresponding histograms given in Figure 2. Further details on the data collection, as well as descriptive statistics of the database, can be found in Yousefpour (2013).

Soil data were obtained from boring logs found in bridge inspection inventories, which included results of in-situ tests, mainly Texas Cone Penetrometer (TCP) tests. Average skin friction (f_u) along piles, pile tip bearing capacity (q_p) and soil friction angle (Φ) were estimated based on TCP values, using the correlation graphs provided by TxDOT (TxDOT 2006). Soil density was also obtained based on the TCP values.

METHODOLOGY

The herein proposed probabilistic method for evaluation of unknown foundations consists of four main stages as illustrated in Figure 3. In Stage I, BC of the bridge piers included in the database (i.e. bridges with "known foundations") is computed; in Stage II, ANN models are trained to establish a relationship between BC and the relevant above-ground bridge parameters such as geometry, load, location, year built etc. Stages III incorporates the ANN models to estimate the BC for a given "unknown foundation", and Stage IV uses the BC estimate to generate probabilistic predictions about the "unknown foundation" characteristics using Bayesian inference. The unknown parameters include foundation type, foundation dimension and embedment depth, average skin friction and tip bearing capacity for piles, as well as cohesion and friction angle for shallow foundations (see Table 2). ANN models and Bayesian inversion codes were developed using MATLAB.

In order to address the possible scenarios regarding data availability about foundation type and soil boring data, four different problems were defined as defined in Table 2. The first index in the problem nomenclature represents the availability of information regarding foundation type and second index represents the soil data availability; 1 means the presence and 0 indicates the absence of data. Table 2 lists the target (unknown) parameters for each scenario.

Load and Bearing Capacity Computation

A simple method was implemented to calculate the dead load of the bridges based on the standard bridge sheets provided by TxDOT (Yousefpour 2013). The total load for a bridge bent was estimated using the standard tables, based on the roadway width and span length, whereas the actual live load for each bridge was calculated based on the standard design vehicle provided by Item 31 of the NBI (see Figure 2).

Based on consultation with local DOT bridge engineers, design procedures provided by TxDOT Geotechnical Manual was determined to be the prevailing method for bridge foundation design in Texas before 2000. This method follows AASHTO (2002a) Allowable Stress Design (ASD) procedure, which has been the prevalent standard guide in the US between 1920 and 2000 (Caltrans 2015). Majority of bridges in the accumulated database were built between 1960 and 2000 (see Figure 2). In addition, majority of UFBs identified through the US are built between 1920 and 2000 (Stein and Sedmera 2006). Therefore, in this study, BC of deep foundations were calculated based on TxDOT Geotechnical Manual. For shallow foundations, AASHTO specifications (AASHTO 2002b) were adopted, as shallow foundations were not allowed to be designed for bridges according to TxDOT Geotechnical Manual. The equations used to calculate allowable bearing capacity are provided below. These are also incorporated as forward models in the Bayesian inversion framework.

$$Q_a = n\varphi_b\left[f_u(dp_{Cn} - d_{scour})4D_{Cn} + q_p {D_{cn}}^2\right] \quad \text{Eq. 1: Concrete Piles}$$

$$Q_a = n\varphi_b[\beta f_u(dp_{Dr} - d_{scour})\pi D_{Dr} + q_p\,(\pi {D_{Dr}}^2/4)] \quad \text{Eq. 2: Drilled Shafts}$$

$$Q_a = n\varphi_b[f_u(dp_{st} - d_{scour})A_{St}/3 + q_p\,A_{St}] \quad \text{Eq. 3: Steel Piles}$$

$$Q_a = \varphi_b\left[\gamma D_f N_q d_q s_q C_{wq} + 0.5\gamma B N_\gamma d_\gamma s_\gamma C_{w\gamma}\right]LB \quad \text{Eq. 4: Spread Footings (Sand)}$$

$$Q_a = \varphi_b\,cN_c d_c s_c LB \quad \text{Eq. 5: Spread Footings (Clay)}$$

Where:

$$N_q = e^{\pi*\tan(\phi)}\frac{1+\sin\phi}{1-\sin\phi}$$

$$d_q = 1 + 2\ \tan\phi\,.\,(1-\sin\phi)^2\tan^{-1}\frac{D_f}{B}$$

$$s_q = 1 + \frac{B}{L}\tan\phi$$

$$N_\gamma = 2(N_q + 1)\tan\phi$$

$$d_\gamma = 1$$

$$s_\gamma = 1 - 0.4\frac{B}{L}$$

$$N_c = 5.14$$

$$d_c\ =\ 1$$

$$s_c = 1 + 0.2\frac{B}{L}$$

ANN Models

Artificial Neural Networks, first introduced by (McCulloch and Pitts 1943), are computational models consisting of parallel inter-connected processing units called neurons. ANNs have emerged from the idea of simulating the brain function in terms of pattern recognition, learning, and generalization. Neurons in ANNs resemble the biological neurons, and connections between them resemble axons and dendrites through which biological neurons transmit and receive signals. Each connection between two neurons holds a weight value, which represents the synapse at the intersection of the axon and dendrites between two biological neurons. Similar to human brain, the process of learning in ANNs is defined as the gradual adjustment of connection weights (synapses in biological neurons) by signals passing through them (Bishop 1995).

ANNs are usually divided into two broad categories in terms of their architecture: feed-forward and recurrent (or feedback networks). In feed-forward networks, the input of each unit in a layer is the output of the units in layer before, while in recurrent networks, the input of a neuron could come from units (neurons) in the latter layer or from itself. Feed-forward networks are memory-less in the sense that their response to an input is independent of the previous network state. Recurrent networks, on the other hand, are dynamic systems.

Learning in ANNs can be considered as updating network architecture and connection weights so that the network can efficiently perform a task. The network is usually trained by presenting a set of input data. ANNs can learn from the underlying rules, like implicit relation between input-outputs, acting as an artificial intelligent model.

Multilayer Perceptron networks (MLPs) are feed-forward neural networks that have been widely used for prediction and approximation. A simple MLP network consists of three layers: an input layer where the input parameters are fed to the network, an output layer which consists of neurons that predict the target parameters, and a “hidden” layer in between, consisting of neurons that connects the input layer’s neurons to the output layer’s. Outputs of the neurons in the hidden layer are not observed in the computation process and are only inputs to the output neurons. This is the reason they are called "hidden neurons". Hidden neurons apply a transfer (often nonlinear) function that maps the input parameters to the target parameters. The learning procedure of MLPs consists of adjusting the weights of the connections between hidden and output layers to minimize an objective function. The objective function is defined as the mean square error of predictions (*MSE*):

$$MSE = \frac{1}{N}\sum_{i=1}^{N}(d_i - y_i)^2 \qquad \text{Eq. 6}$$

where d_i is the actual value of the target parameter, and y_i is the estimated value by the ANN model, and *N* is the number of training examples presented to the network.

MLP models were developed and trained using the accumulated database to predict the BC of bridge foundations. Comprehensive analyses were performed on the architecture of the MLP networks and showed that a single hidden layer including 20 neurons with tan-sigmoid activation function was the optimum architecture (Yousefpour, 2013). Figure 4 shows the architecture of the implemented MLP network.

The input parameters selected for BC estimation are those incorporated in the design of bridge foundations, including dead load, live load, soil resistance parameters, year built, and location (county, latitude and longitude), as presented in Table 3. In other words, the selection of input parameters was based on the physics of limit state equilibrium of foundation under vertical loads. The relationships below shows that allowable BC (Q_a) is linearly related to loads (DL and LL).

$$\gamma_1 DL + \gamma_2 LL = Q_a \qquad \text{Eq. 7}$$

Where γ_1, γ_2 are load factors from applicable standards.

Allowable BC is linearly correlated with average skin friction (as shown in Table 3), which itself is directly correlated with average TCP. Many of UFBs are old, or designed by random agencies, therefore it is not clear what standard (and factors) was used for their design. Also, standards (and factors) vary over the years and across various locations, depending on typical design and construction methods. Location and County can also provide inherent information on geological conditions at a bridge (such as rock depth where piles/shafts are normally designed to sit on with a minimum socket length). These all were the reasons for incorporating year built, location, and county as inputs into the ANN models in addition to load and soil resistance parameters.

The aim was to allow ANNs to implicitly learn the adopted load and resistance factors (or overall factor of safety in case of ASD method) at the time of design from the collected database of bridges and later generalize it to a new, unseen bridge to estimate the BC. For cases where soil data was not available, the soil resistance parameters were removed from the input layer.

It should be noted that a wider range of parameters were considered in preliminary ANN models and networks with various combination of parameters were compared to ensure the most relevant parameters were eventually selected for BC prediction.

The MLP networks weights and biases were adjusted using the Back-Propagation algorithm incorporating the Levenberg-Marquardt optimization method (Bishop 1995). The performance of the proposed ANN models was assessed using R^2 and *RMSE* (Root Mean Squared Error). The random subsampling method (Monte-Carlo Cross Validation) was performed by iteratively sampling data points for training (60%), validation (20%), and testing (20%) datasets, generating a new network during each iteration (Picard and Cook 1984).

The ANN models were trained using the corresponding training datasets and their performance was monitored against the validation datasets. Training was stopped when one of the following criteria is reached; minimum error (0), maximum number of iterations (1000), minimum gradient of error function (1E-10), or when the validation error started to increase monotonically (more than five successive validation failures). The performance of the networks was examined using the test datasets that had not been presented to the ANN models during the training process. Ten thousand networks were generated using the random subsampling method to form an ensemble of MLP networks for prediction of BC. The networks with $R^2 < 0.8$ over the test datasets were removed from the ensemble, assuming networks with $R^2 \geq 0.8$ generate reasonably accurate predictions. Ultimately, ten ensembles of the MLP networks were developed to predict BC based on the availability of soil and foundation type information, named as MLP-BC*11*, MLP-BC*10*, MLP-BC*01*-Conc, MLP-BC*01-DrSh*, MLP-BC*01-Steel*, MLP-BC*01-Spread,* and MLP-BC*00-Conc,* MLP-BC*00-DrSh,* MLP-BC*00-Steel,* MLP-BC*00-Spread*.

Bayesian Inference

Bayesian inference provides a methodology to update the probability of an event or a variable when new evidence becomes available. This method has been already employed as a powerful tool in a number of geo-applications including site characterization, soil parameter estimation, inverse analysis of embankments, liquefaction potential assessment, evaluation of geotechnical model uncertainties, calibration of soil constitutive models, and land slide analysis (Cividini et al. 1983; Honjo et al. 1994; Juang et al. 2002; Rechenmacher and Medina-Cetina 2007; Medina-Cetina and Nadim 2008; Zhang et al. 2009; Ranalli et al. 2010, Medina-Cetina and Esmailzadeh 2014). According to the Bayes' paradigm, considering $\boldsymbol{\theta} = \{\theta_1, \cdots, \theta_k\}$, a vector of model parameters, and $\mathbf{d}_{obs} = \{d_1, \cdots, d_n\}$, a vector of new observations about the process of interest, then $p(\boldsymbol{\theta})$ represents the prior distribution, $f(\boldsymbol{d}_{obs}|\boldsymbol{\theta})$ represents the likelihood function, and $p(\boldsymbol{\theta}|\boldsymbol{d}_{obs})$, the posterior distribution can be computed as (Robert 2007; Hoff 2009):

$$\mathrm{p}(\boldsymbol{\theta}|\mathbf{d}_{obs}) = \frac{\mathrm{p}(\boldsymbol{\theta}) f(\mathbf{d}_{obs}|\boldsymbol{\theta})}{\int \mathrm{p}(\boldsymbol{\theta}) f(\mathbf{d}_{obs}|\boldsymbol{\theta}) d\boldsymbol{\theta}} \qquad \text{Eq. 8}$$

The denominator of the above equation is a normalizing constant; thus, the posterior distribution is proportional to the prior times the likelihood:

$$\mathrm{p}(\boldsymbol{\theta}|\mathbf{d}_{obs}) \propto \mathrm{p}(\boldsymbol{\theta}) f(\mathbf{d}_{obs}|\boldsymbol{\theta}) \qquad \text{Eq. 9}$$

There are several methods to draw samples from posterior probability distributions. The Markov-Chain Monte-Carlo method (MCMC) using the Metropolis-Hastings algorithm was implemented in this study (Hoff 2009).

Prior Distributions

The unknown parameters of bridge foundations, and soil properties were considered as random variables, and for each a prior distribution was defined based on the empirical distributions generated from the accumulated database. In particular, lognormal distributions were found to be a good fit to represent all the unknown parameters except for Foundation Type (*FT*). For *FT* prior distribution, the empirical distribution of bridge foundation types in the region was adopted. *FT* was a discrete variable taking values 1 to 4 representing concrete piling, drilled shafts, steel piling, and spread footing, respectively.

Likelihood Function

The likelihood is defined as the probability density function of the observations given the model parameters, which is formulated as the discrepancy between model predictions (d_{pred}) and observations (d_{obs}) (prediction error).

While not presented here, the distribution of error between the ANN-estimated BC and BC estimated from analytical equations for "known foundations", can be shown to follow a Normal distribution. Considering the analytical bearing capacity equations (Eq. 1 to 5) as the forward models [$Q_a(\boldsymbol{\theta})$], and the predicted BC by the ANN models (BC_{ANN}) as the only observation for a particular foundation, the likelihood function can be written as:

$$f(d_{obs}|\boldsymbol{\theta}) = \frac{1}{\sigma\sqrt{2\pi}} \exp\left[-\frac{(d_{obs}-d_{pred}-b)^2}{2\sigma^2}\right] = \frac{1}{\sigma\sqrt{2\pi}} \exp\left[-\frac{(Q_a(\boldsymbol{\theta})-BC_{ANN}-b)^2}{2\sigma^2}\right] \qquad \text{Eq. 10}$$

where b is the mean (bias) and σ is the standard deviation of the normal distribution for error and can be either assessed as hyper-parameters or obtained from the corresponding ANN models.

Implementation Steps

The flowchart in Figure 5 outlines the implementation steps of the proposed probabilistic method for evaluating UFBs. These steps are described below:

S*tep 1: Data Mining.* The parameters (items) required for implementing the probabilistic approach are retrieved from the NBI and from bridge inspection inventories. Further details on the description of each item can be found in the TxDOT's coding guide (Weseman 1995). For a bridge interior bent (pier) these parameters are used as input data for the ANN models to estimate the BC:

- Item 3: County
- Item 16: Latitude
- Item 17: Longitude
- Item 27: Year built
- Item 31: Design load
- Item 34: Bridge skew
- Item 44.1-D1: Substructure type above ground for main spans
- Item 46: Total number of spans in bridge
- Item 48: Max span length
- Item 51: Roadway width
- Average TCP and skin friction along the piles (from soil boring data, if available)
- Average span length for the bent (from bridge construction/inspection plans)

Step 2: Assessment of Dead and Live Loads. Loads are calculated following the method described earlier (See Load and Bearing Capacity Calculation Section) and using TxDOT standard bridge design sheets (Yousefpour, 2013).

Step 3: Identification of above-ground Foundation Properties. The above-ground properties of the bridge foundation, such as type, dimension and number of piles/shafts in the bent are identified, if possible.

Step 4: Prediction of Bearing Capacity Using the ANN Models. Depending on information availability for soil boring data and the foundation type, the subsequent sub-steps are followed for estimating the expected BC for a bridge interior bent:

Step 4-1: If foundation type is unknown and soil boring data is unavailable, predict the BC using the ANN model, MLP-BC00.

Step 4-2: If foundation type is unknown but the soil boring data is available:

Step 4-2-1: Compute the average TCP value and average ultimate skin friction (f_u) along the foundation from the nearest borehole data.

Step 4-2-2: Predict the BC using ANN model, MLP-BC01.

Step 4-3: If both foundation type and soil boring data are available:

Step 4-3-1: Compute the average ultimate skin friction (f_u) and the average TCP value along the foundation from the nearest borehole data.

Step 4-3-2: Implement the ANN model, MLP-BC11 for the corresponding foundation type to predict the BC.

Step 4-4: If the foundation type is known but the soil boring data is unavailable, predict the BC using the ANN model, MLP-BC10 for the corresponding foundation type.

Step 5: Bayesian Inversion. Draw samples from the joint posterior distribution of the foundation type, foundation dimensions, and soil resistance parameters using MCMC (unknown parameters as defined in Table 2).

RESULTS

ANN Models for Bearing Capacity Prediction

The predicted BC using ANN models vs. the calculated BC using the analytical equations for bridge piers in the test dataset are presented in Figure 6. For each bridge pier foundation, red dots, vertically scattered, represent predictions by the networks in an ensemble, and the dark circles show the averaged value over all network predictions.

The performance of the models can be compared through both the R^2 and *RMSE* of the averaged predictions (the R^2 and *RMSE* presented for each model correspond to the average of the predictions). By comparing MLP-BC10 (foundation type is known, soil boring is not available) with MLP-BC11 models (foundation type is known, soil boring is available), it is observed that adding the soil strength parameters into the ANN model inputs, improves the accuracy of bearing capacity estimations. *RMSE* of the models reduced after inputting the soil parameters, in the order of 25% for concrete piles, 33% for drilled shafts, 55% for steel piles, and 27% for spread footings.

The order of magnitude for average R^2 was around 0.8 or above for all models, except for MLP-BC-Spread. This indicates that these models were able to learn from the examples in the training dataset and then make reasonably accurate predictions for new cases in the test dataset. Due to the limited amount of data for bridges with spread footings, the MLP-BC-Spread model could not generate predictions as accurate as the other models.

Validation of the Probabilistic Method - Case Study

In order to validate the proposed probabilistic method, a case study was performed on a bridge with available as-built plans and substructure information located in the Bryan District. The bridge was located a mile south of FM 485, founded on drilled shafts over the Big ELM Creek and was analyzed under four possible scenarios: Problems *11*, *10*, *01* and *00*. Table 4 shows the actual values for the foundation of the interior pier, extracted from as-built plans and the inspection database. Drilled shafts are 37 ft (11.3 m) deep, with 30 in (76 cm) diameter. The BC was first predicted by the ANN models, and then the foundation and soil characteristics were estimated through MCMC simulations and compared against the actual values.

Problem 11 (Foundation Type Known, Soil Boring Data Available), Unknown Parameter: dp_{Dr}

This inversion process included one million MCMC simulations. Figure 7 illustrates how the cumulative mean and standard deviation of the MCMC sampling process converge for pile depth (dp_{Dr}). The convergence analysis plots indicate that the Markov chain achieved a stationary condition approximately after the 200,000 simulations, the point after which the posterior is populated.

Figure 8 shows the empirical prior and marginal posterior Probability Density Functions (PDF) of dp_{Dr} generated from MCMC simulations. Various probabilistic inferences can be made from the posterior CDF. One of the useful inferences is the probability of non-exceedance for a specific embedment depth, for e.g. the minimum required embedment depth considering the maximum estimated scour depth, based on which the probability of failure due to scour can be estimated. Figure 8 also shows the effect of the new evidence, i.e. the BC estimate by the ANN model on the state of the current evidence about the foundation depth (prior distribution). This effect is reflected in the reduction of the standard deviation of the foundation depth (i.e. higher confidence in determination of the foundation depth).

Table 5 presents the expected value (E), standard deviation (Std), 95% confidence interval ($CI_{95\%}$), the mode value and the 10th quantile of the posterior distribution. It can be observed that the mean and mode of the posterior distribution of dp_{Dr} (13.5 m and 12.9 m respectively) are close to the actual pile depth of 11.3 m, with a standard deviation of 2.6 m. The 10th quantile can be taken as a conservative estimate on the minimum embedment depth for evaluating scour failure risk at the bridge pier.

Problem 10 (Foundation Type Known, Soil Boring Data Not Available), Unknowns: dp_{Dr}, q_p, and f_u

One million MCMC simulations were performed considering the scenario of Problem *10*. The CDF of the prior and marginal posterior distributions of the shaft depth (dp_{Dr}), as well as the skin friction (f_u) and point bearing capacity at tip of the shaft (q_p) are presented in Figure 9.

Table 6 provides the statistics of the posterior distributions. The mean of the marginal posterior distributions for dp_{Dr} is reasonably close to the actual value (11.7 versus 11.3 m). As compared to Problem11, the uncertainty in predictions of the shaft depth is higher (standard deviation of 3.2 m compared to 2.6 m) due to lack of information regarding soil parameters. It should be noted that although the mean of the posterior predictions is slightly closer to the actual values in this scenario, the uncertainty has increased as reflected in the increase in standard deviation and the confidence interval. The $CI_{95\%}$ for embedment depth is [8.9 18.8] for Problem 11, whereas for Problem 10, it is [6.7 19], showing an increase in the range of likely values.

Also, comparing prior with posterior distributions, it is observed that the uncertainty of the parameters is reduced by introducing the *BC* estimate of the foundation (i.e. greater confidence on the assessment of likely unknown foundation parameters). Also, the mean and mode of the posterior distributions approach to the actual values for the three parameters.

The joint posterior distributions of the three parameters are shown in Figure 10. A negative correlation, as expected, is observed between the shaft depth versus skin friction, and the shaft depth versus tip bearing capacity. A similar trend was also observed between skin friction and tip bearing capacity showing that in softer soil, foundations need to go deeper to achieve the required capacity.

Problem 01 (Foundation Type Unknown, Soil Boring Data Available), *Unknown Parameters:* FT, dp_{Cn}, D_{Cn}, dp_{Dr}, D_{Dr}, dp_{St}, A_{St}, B, L, D_f

Problem *01* required two million MCMC simulations due to the increasing number of unknown foundation parameters. Since the foundation type (*FT)* is unknown, the sampling value of *FT* conditioned the sampling of other parameters. Figure 11 shows the prior versus marginal posterior distribution of *FT.* The probability of *DrSh*, which is the actual foundation type, increases in the posterior distribution compared to the prior distribution, as opposed to the other foundation types. The significant shift of probability from *Conc* to *DrSh* (a decrease from 70% to 45% for *Conc* and an increase from 20% to 50% for *DrSh*) between prior and posterior distributions correctly indicates that the foundation is drilled shaft. Steel piling and spread footing both show very unlikely to be the actual foundation type. Figure 12 presents the joint posterior probability distributions of embedment depth and dimension for *DrSh* and *Conc*. Also, Table 7 summarizes the statistics of the posterior distributions for the unknown parameters. These estimates show that the mean of the marginal posterior distributions for dp_{Dr} and D_{Dr} (13.5 m and 85 cm) are reasonably close to the actual values of the shaft depth and diameter (11.3 m and 76 cm, respectively).

Problem 00 (Foundation Type Unknown, Soil Boring Data Not Available), *Unknowns:* FT, dp_{Cn}, D_{Cn}, dp_{Dr}, D_{Dr}, dp_{St}, A_{St}, B, L, D_f, f_u, q_p, φ

This problem type represents the worst-case scenario where there is no information available regarding the foundation type and soil parameters. Two million samples were generated via MCMC simulations to populate the corresponding posteriors. By looking at the *FT* simulations, it is observed that only a few number of samples of *FT=Spread* are accepted through the MCMC simulations, which indicates that the foundation is very unlikely to be a spread footing. Figure 13 compares the prior and posterior distributions for *FT*. Unlike the previous scenario, in this case, the probability for *Conc* is the highest, followed by *DrSh. Steel* and *Spread* show much lower probabilities. However, similar to Problem *01* scenario, when comparing posterior versus prior probabilities, *DrSh* shows a significant increase whereas *Conc* shows a significant decrease in probability. This is an indication that the foundation type is drilled shaft, although the "most likely" foundation type according to posterior can be inferred as concrete piling. Nevertheless, the engineering judgment in such case should be to consider both possibilities for the foundation type.

Figure 14 presents the joint posterior probability distributions for the foundation depth versus foundation size and soil resistance parameters for *DrSh* and *Conc*. The negative correlation between depth and soil resistant parameter is captured in the joint distributions of dp_{Dr} with f_u and q_p. Table 8 provides the statistics for the unknown parameters obtained from the corresponding marginal posterior distributions. The mean of the posterior distributions for dp_{Dr} and D_{Dr} (12.7 m, 82 cm) is reasonably close to the actual values of the shaft depth and diameter (11.3 m and 76 cm). Also, if the actual foundation type is considered as concrete piling, the mean of the posterior distributions for dp_{Cn} appears to provide a reasonable, conservative estimate of foundation embedment (~9 m) for scour evaluations.

Comparing Problem 01 with 00 (scenarios where the *FT* is unknown), removing soil resistance parameters and introducing them as unknowns resulted in reduction of the probability of drilled shaft (from 49% to 38%) and increased the uncertainty in predictions in that manner. The large number of unknowns (9 for Problem 01 and 13 for Problem 00) and having only one observation (the estimate of BC) resulted in only a small reduction of uncertainty in posterior distributions with respect to prior distribution (see Figure 15). Subsequently, in such problem scenario where the foundation type is unknown, adding soil parameters as additional unknowns in Problem 00 did not significantly influence the uncertainty in embedment depth predictions, therefore the standard deviation and confidence interval of the posterior distributions are not very different between Problem 01 and 00.

Summary of Results and Discussions

Figure 15 presents the 95% confidence interval (points at either side) and mean (middle point) of the prior versus posterior distributions for the embedment depth, obtained under the four problem scenarios. This diagram better shows how uncertainty is reduced from the prior to the posterior distributions through Bayesian inference. It is also easy to compare the scenarios and how uncertainty increases from Problem 11 to Problem 00, as more unknowns are added to the problem. It should be noted that in this study the prior distributions are defined based on collected data for bridges (informative priors), which significantly influence the inversion results. The significance of uncertainty reduction through Bayesian inference would have been more evident if non-informative (uniform) priors were assumed instead (e.g. to assume that nothing is known about the model parameters). The more limited available data is, the more significant the uncertainty reduction through the Bayesian approach.

In general, Bayesian formulation provided reasonable unbiased estimations for all problem scenarios. Limited benefits in terms of uncertainty reduction was achieved in scenarios where foundation type was assumed to be unknown. Having said that, reasonable inferences regarding the likely foundation type can still be made in such scenarios.

CONCLUSIONS

A new probabilistic methodology was developed in this study, incorporating estimates of bearing capacity predicted by ANN ensemble models and Bayesian inference framework for a full probabilistic characterization of unknown bridge foundations. Unlike the deterministic solution proposed by the authors (Yousefpour et al. 2014), the probabilistic solution here aims at providing a transparent and systematic assessment of uncertainty of model parameters and predictions for unknown foundations.

ANNs proved successful in predicting the bearing capacity of bridge foundations, based on superstructure characteristics, loading, soil strength, location, and year built. The fundamental of training the ANN models for estimating BC was based on principles of limit equilibrium. Including non-physics-based properties such as location and year built resulted in more accurate evaluations of bearing capacity due to their inherent correlation with applicable designs methods and standards, local geology, and adopted safety factors.

It was shown that based on the available evidence (collected data) and conditioned on the estimate of BC from the developed ANN models, probability distributions can be generated for the unknown parameters of a bridge foundation through Bayesian inversion and MCMC simulations. A step by step guideline was provided to show the implementation of the proposed probabilistic method to infer the type, embedment depth, and dimension of an unknown bridge foundation. The method was validated based on a case study on an actual bridge with hypothetically unknown foundation. Results showed that the generated posterior distributions can provide reasonable estimations for expected foundation type and embedment depth under varying evidence scenarios, as well as measures of uncertainty and confidence, which allow for systematic scour risk evaluations.

For scenarios where foundation type was unknown, it was possible to determine the actual foundation type based on the observed changes in the posterior distribution in comparison with the empirical prior distribution. However, determining the actual foundation type solely based on the maximum posterior probability showed to be misleading. This occurred only for the worst-case scenario with no information on foundation type and soil, resulting in 13 unknown parameters. This large number of unknowns increased the uncertainty in the Bayesian inversion results and consequently in determining the actual foundation type. It should be noted that in most cases the foundation type can be inferred from in-situ inspections and simple field tests. Therefore, it is highly recommended to first determine the foundation type and then implement the proposed method to infer the foundation embedment depth for scour risk assessments.

Overall, this study introduced a rigorous, evidence-based method for probabilistic evaluation of unknown foundations at a much lower cost compared to existing in-situ test methods. This method can be adopted by transportation authorities (e.g. US DOTs) to predict the minimum foundation embedment depth for evaluating scour vulnerability of bridges with unknown foundations. The probabilistic inferences and confidence estimates derived using this method can also facilitate risk assessments and decision-making for implementing countermeasures and plans of action.

Scope of Use, Assumptions, and Limitations

The following points should be considered for adopting the proposed methodology for evaluating bridges with unknown foundations:

- ANN models shall be trained with sufficient collected data from the regional population of bridges.
- ANN models shall not be used to make predictions on a bridge outside the range the training database.
- The design codes and standards have been changing over decades. In fact, very old bridges may not have been designed based on a particular code at all. The equations used herein for BC estimations was based on the ASD method which was prevalent in the US between 1970 to 2000. Since most of the identified UFBs were built before 2000, these equations were considered applicable to majority of these bridges.
- In general, there is a significant variability in foundation design and construction methods for bridges across various locations, ground conditions, and year of built. These variabilities introduce both bias and uncertainty in the estimates of BC for bridges in the training database as the target parameter and later on in the predictions of BC by ANN models for an unknown foundation. The bias and uncertainty can be quantified (as hyperparameters) through Bayesian inference and reflected in the posterior probability distributions of foundation depth and dimensions.

DATA AVAILABILITY STATEMENT

Some or all data, models, or code generated or used during the study are proprietary or confidential in nature and may only be provided with restrictions. Sample data and codes can be provided upon request.

ACKNOWLEDGMENTS

This project was sponsored by the TxDOT. The Authors thank John Delphia for all his technical support throughout the development of the project. The authors are especially indebted to Keyvon Jahedkar (RIP) and Anthony Garcia from the TxDOT Bryan District, for their assistance in collecting bridge information. The valuable help of Mark McClelland on load calculations and Brittany Hanley on populating and processing the database are also greatly appreciated.

NOTATIONS

A_{St}: Cross sectional area of steel piles, perimeter length ~1/3 of cross section area

B: Footing width

$C_{wq}, C_{w\gamma}$: Correction factors for groundwater depth

c: Cohesion

D_{Cn}: Dimension of squared concrete piles

D_{Dr}: Diameter of drilled shafts

D_f: Footing embedment depth

$d_c,\ d_\gamma,\ d_q$: Depth correction factors

dp_{Cn}: Embedment depth of concrete piles

dp_{Dr}: Embedment depth of drilled shafts

dp_{st}: Embedment depth of steel piles

$d_{scour} = 1$m: Disregarded pile embedment depth to account for scour

f_u: Skin friction of piles

L: Footing length

$N_c,\ N_q,\ N_\gamma$: Bearing capacity factors

n: Number of piles per pier (bent)

Q_a: Allowable bearing capacity

q_p : Tip bearing capacity of piles

$S_c,\ S_q,\ S_\gamma$: Shape correction factors

$\beta = 0.7$: Skin friction reduction factor for soil disturbance during drilling

Φ: Soil internal friction angle

$\varphi_b = 0.5$: Resistance factor

γ: Soil unit weight

REFERENCES

AASHTO (2002a). "AASHTO Standard Specifications for Highway Bridges." Washington, D.C., American Association of State Highway and Transportation Officials.

AASHTO (2002b). "LRFD Highway Bridge Design Specifications." Washington, D.C., American Association of State Highway and Transportation Officials,.

Bateni S. M., Borghei, S. M. and Jeng, D. S. (2007). "Neural Network and Neuro-Fuzzy Assessments for Scour Depth around Bridge Piers." *Engineering Applications of Artificial Intelligence*, 20(3), 401-414.

Bishop C. M. (1995). *Neural Networks for Pattern Recognition*. Clarendon Press, Oxford University Press, Oxford.

Briaud J.-L., Medina-Cetina, Z., Hurlebaus, S., Everett, M., Tucker, S., Yousefpour, N. and Arjwech, R. (2011). "Unknown Foundation Determination for Scour." Report No. FHWA/TX-12/0-6604-1,Texas Department of Transportation and Federal Highway Adminstration.

Caltrans (2015), Bridge Design Practice, California Department of Transportation.

Cividini A., Maier, G. and Nappi, A. (1983). "Parameter estimation of a static geotechnical model using a Bayes' approach." *International Journal of Rock Mechanics and Mining Sciences & Geomechanics Abstracts*, Elsevier.

Demuth H., Beale, M. and Hagan, M. (2009). "MATLAB Neural Network Toolbox User's Guide." The MathWorks.

FHWA (2011). "Unknown Foundations." U.S. Department of Transportation.

Hoff P. D. (2009). "A first course in Bayesian statistical methods." Springer.

Honjo Y., Wen-Tsung, L. and Guha, S. (1994). "Inverse analysis of an embankment on soft clay by extended Bayesian method." *International Journal for Numerical and Analytical Methods in Geomechanics*, 18(10), 709-734.

Juang C. H., Jiang, T. and Andrus, R. D. (2002). "Assessing probability-based methods for liquefaction potential evaluation." *Journal of Geotechnical and Geoenvironmental Engineering*, 128(7), 580-589.

Kaya A. (2010). "Artificial Neural Network Study of Observed Pattern of Scour Depth around Bridge Piers." *Computers and Geotechnics*, 37(3), 413-418.

Lee T. L., Jeng, D. S., Zhang, G. H. and Hong, J. H. (2007). "Neural Network Modeling for Estimation of Scour Depth around Bridge Piers." *Journal of Hydrodynamics, Ser. B*, 19(3), 378-386.

Maser K. R., Sanayei, M., Lichtenstein, A. and Chase, S. B. (1998). "Determination of bridge foundation type from structural response measurements." *Non-Destructive Evaluation Techniques for Aging Infrastructure & Manufacturing*, International Society for Optics and Photonics.

McCulloch W. and Pitts, W. (1943). "A Logical Calculus of the Ideas Immanent in Nervous Activity." *Bulletin of Mathematical Biology*, 5(4), 115-133

Mclemore S., Zendegui, S., Whites, J., Sheppard, M., Gosselin, M., Demir, H., Passe, P. and Hayden, M. (2010). "Unknown Foundation Bridges Pilot Study." Federal Highway Administration & Florida Department of Transportation.

Medina-Cetina Z. and Esmailzadeh S. (2014), "Joint States of Information from Different Probabilistic Soil Profile Reconstruction Methods," *Georisk,* 8 (3), 171-191.

Medina-Cetina Z. and Nadim, F. (2008). "Stochastic design of an early warning system." *Georisk*, 2(4), 223-236.

Mercado E. and O'Neill, M. (2003). "Methods to measure scour depth and the depth of unknown foundations." *The 3rd International Conference on Applied Geophysics-Geophysics 2003*.

Olson L. (2005). "Dynamic Bridge Substructure Evaluation and Monitoring." FHWA.

Olson L., Jalinoos, F. and Aouad, M. F. (1998). "Determination of Unknown Subsurface Bridge Foundations: NCHRP 21-5 Interim Report Summary." FHWA.

Picard R. R. and Cook, R. D. (1984). "Cross-Validation of Regression Models." *Journal of the American Statistical Association*, 79 (387), 575-583.

Ranalli M., Gottardi, G., Medina-Cetina, Z. and Nadim, F. (2010). "Uncertainty quantification in the calibration of a dynamic viscoplastic model of slow slope movements." *Landslides*, 7(1), 31-41.

Rechenmacher A. L. and Medina-Cetina, Z. (2007). "Calibration of soil constitutive models with spatially varying parameters." *Journal of Geotechnical and Geoenvironmental Engineering*, 133(12), 1567-1576.

Rix G. J. (1995). "Interpretation of nondestructive tests on unknown bridge foundations using artificial neural networks." *Nondestructive Evaluation of Aging Structures and Dams*, 2457, 102-112.

Robert C. (2007). "The Bayesian choice: from decision-theoretic foundations to computational implementation." Springer Verlag.

Robinson B. and Webster, S. (2008). "Successful testing methods for unknown bridge foundations." *Proceedings of The Fifth Highway Geophysics NDE Conference, Charlotte, NC*.

Sayed S. M., Sunna, H. and Moore, P. R. (2011). "Re-Classifying Bridges with Unknown Foundations." 5th international conference on scour and erosion. San-Francisco, CA.

Stein S. and Sedmera, K. (2006). "Risk-Based Management Guidelines for Scour at Bridges with Unknown Foundations." Springfield,VA, National Cooperative Highway Research Program (NCHRP)**,** Project 24-25.

TxDOT (2002). "Bridge Inspection Manual." Texas Department of Transportation.

TxDOT (2006). "Geotechnical Manual." Texas Department of Transportaion (TxDOT).

Weseman W. A. (1995). "Recording and Coding Guide for the Structure Inventory and Appraisal of the Nation's Bridges." Washington D.C., Office of Engineering.

Yousefpour N. (2013). "Comparative Deterministic and Probabilistic Modeling in Geotechnics: Applications to Stabilization of Organic Soils, Determination of Unknown Foundations for Bridge Scour, and One-Dimensional Diffusion Processes." Ph.D. Dissertation, Texas A&M University, College Station, Texas.

Yousefpour N., Medina-Cetina, Z. and Briaud, J.-L. (2014). "Evaluation of Unkown Foundations of Bridges Subjected to Scour using Artificial Neural Networks." *Transportation Research Record: Journal of the Transportation Research Board*, 2433, 27-38.

Zhang J., Zhang, L. and Tang, W. H. (2009). "Bayesian framework for characterizing geotechnical model uncertainty." *Journal of Geotechnical and Geoenvironmental Engineering*, 135(7), 932-940.

Zounemat-Kermani M., Beheshti, A. A., Ataie-Ashtiani, B. and Sabbagh-Yazdi, S. R. (2009). "Estimation of Current-Induced Scour Depth around Pile Groups using Neural Network and Adaptive Neuro-Fuzzy Inference System." *Applied Soft Computing*, 9(2), 746-755.

LIST OF TABLES

TABLE 1. Main bridge characteristics included in the working database

Item/Parameter	No	Min	Max	Mean	Median	Std. Dev.
County$^+$: Item 3	1	21	239	-	145	-
Latitude (deg): Item 16	2	30.06	31.97	30.88	30.85	0.45
Longitude (deg): Item 17	3	95.4	97.25	96.27	96.25	0.4
Function Class$^+$: Item 26	4	1	25	-	4	-
Year Built: Item 27	5	1922	2009	1964	1961	20
Average Annual Daily Traffic: Item 29	6	20	31070	4470.33	1900	5445.38
Design Load$^+$: Item 31	7	0	5	-	4	-
Bridge Skew (deg): Item 34	8	0	99	4.59	0	12.2
Superstructure Type for Main Span$^+$: Item 43-1	9	1102	2126	-	1125	-
Substructure Type above Ground for Main Span$^+$: Item 44-1-D1	10	1	7	-	1	-
Item 44-1-D2: Substructure Type below Ground for Main Span$^+$	11	1	8	-	2	-
Total Number of Spans: Item 46	12	1	44	5.4	4	4.9
Max Span Length (m): Item 48	13	10	240	39.7	30	25.5
Roadway Width (m): Item 51	14	19	90	34.45	33.5	12.3
Waterway Adequacy$^+$: Item 71	15	1.1	9	-	6	-
Deck Type for Main Span$^+$: Item 107-1	16	1	2	-	1	-

Average TCP along Pile (Avg. TCP) (blows/ft)*	17	10.5	1414.8	134.5	98.7	141.8
Skin Friction (f_u) (MPa)	18	0.03	1.94	0.21	0.17	0.17
TCP at Pile Tips (Point TCP) (blows/ft)*	19	10	2400	228.6	283.7	269.6
Tip Bearing Capacity (q_p) (MPa)	20	0.06	12.1	2.30	2.60	2
Pile Embedment Depth (d_p) (m)	21	3.1	26	9.4	9	3.6
Footing Width (B) (m)	22	1.2	1.8	1.8	1.6	0.3
Footing Length (L) (m)	23	1.8	27.4	11.3	13.0	11.0
Footing Embedment Depth (D_f) (m)	24	0.0	1.4	0.7	0.8	0.5
Soil Friction Angle (Φ) (deg)	25	30	50	46.5	43.3	7.6
Cohesion (c) (MPa)	26	0.23	0.54	0.35	0.36	0.1
Dead Load (kN)	27	62.4	10328.4	1997.1	1317.7	1888.6
Live Load (kN)	28	229.7	1324.4	474.4	411.5	250.6

* The equivalent value of TCP for 1ft of penetration was calculated for TCP=100 with less than 1ft penetration.

+ Unit-less indices, index values based on NBI coding guide, see Figure 2.

TABLE 2. Definition of problem types based on possible scenarios

Problem Type	**Definition**	**Target (Unknown) Parameters**
Problem 11	Foundation type is known, and soil boring data is available	dp
Problem 10	Foundation type is known, but soil boring data is not available	dp, f_u, q_p
Problem 01	Foundation type is unknown, but soil boring data is available	FT, dp_{Cn}, dp_{Dr}, dp_{St}, D_f, D_{Cn}, D_{Dr}, A_{St}, B, L

Problem 00	Foundation type is unknown, and soil boring data is not available	FT, dp_{Cn}, dp_{Dr}, dp_{St}, D_f, D_{Cn}, D_{Dr}, A_{St}, B, L, f_u, q_p, Φ, c

TABLE 3. Input parameters of MLP models for BC prediction.

Parameter	Min	Max	Mean	Std. Dev.	Median
Load Elements					
Dead Load (per bent) (kN)	562.3	10,324.8	1,824.22	1,687.4	1,312.4
Live Load (per bent) (kN)	229.5	1,323.	449.0	223.9	409.9
Soil Properties					
Ave. TCP (blows/ft)	10.5	1,414.8	140.8	149.9	107.4
Skin Friction* (kPa)	28.7	1943.0	207.5	170.3	166.6
Location and Time					
County+	21	239	-	-	154
Year Built	1925	2008	1969	25	1963
Latitude (deg)	30.0	32.0	30.9	0.5	30.8
Longitude (deg)	95.4	97.3	96.2	0.5	96.2

* Skin friction is the weighted average of skin friction along the depth of the pile

+ See histograms of Figure 2 for code definitions

TABLE 4. Foundation parameters and BC for Big ELM bridge

Parameter	Value
FT	1 (DrSh)
D_{Dr}	76 cm (30 in)
dp_{Dr}	11.3 m (37 ft)
n	3
q_p	3,260 kPa (34 tsf)
f_u	157 kPa (1.6 tsf)
γ	25 kN/m^3 (0.075 tcf)
ϕ	30 deg

BC_{ANN}	6,640 kN (745 tons)
Q_a	5,475 kN (615 tons)

TABLE 5. Statistics of the posterior distribution of the unknown parameter - Problem*11*

Statistics	**Value**
dp_{Dr} (m)	
E	13.5
Std	2.6
$CI_{95\%}$	[8.9 18.8]
Mode	12.90
10^{th} quantile	10.3

TABLE 6. Statistics of the posterior distributions of the unknown parameters - Problem*10*

Parameter / Statistics	***dp_{Dr}(m)***	***f_u(kPa)***	***q_p(kPa)***
E	11.7	229	4,194
Std	3.2	9	2,088
$CI_{95\%}$	[6.7 19]	[91 463]	[1180 91,66]
Mode	12.6	190	3,298
10^{th} quantile	8	123	1,826

TABLE 7. Statistics of the posterior distributions of the unknown parameters - Problem*01*

Parameter / Statistics	***FT=1 (Conc)***		***FT=2 (DrSh)***	
	dp_{Cn} (m)	***D_{Cn} (cm)***	***dp_{Dr} (m)***	***D_{Dr} (cm)***
E	9.2	38.4	13.5	84.7
Std	2.6	2.3	3.5	13.5
$CI_{95\%}$	[5.1 15.1]	[34 43.2]	[7.7 21.4]	[60.8 113.5]

Mode	9.7	38.4	10.6	80.2
10^{th} quantile	6.2	35.4	9.3	68.0

TABLE 8. Statistics of posterior distributions of the unknown parameters - Problem*00*

Parameter / Statistics	dp_{Cn} *(m)*	D_{Cn} *(cm)*	f_u *(kPa)*	q_p *(kPa)*
FT=1: Conc				
E	8.8	38.3	310	6,591
Std	2.4	2.3	187	5,559
CI 95%	[5 14.3]	[34 42.8]	[76 788]	[874 21,628]
Mode	10.7	35.8	230	1,691
10th quantile	6.0	35.4	119	1,630
FT=2: DrSh				
Parameter / Statistics	dp_{Dr} *(m)*	D_{Dr} *(cm)*	f_u*(kPa)*	q_p*(kPa)*
E	12.7	81.8	212	4261
Std	3.4	12.6	113	3245
CI 95%	[7.3 20.4]	[59.8 109.1]	[60 495]	[728 12,030]
Mode	16.9	94	120	6,735
10th quantile	8.7	66.3	91	1,315

LIST OF FIGURES

Figure 6. Predictions of BC by MLP ensembles a) MLPBC00, b) MLPBC01, c) MLPBC10-Conc, d) MLPBC11-Conc, e) MLPBC10-DrSh, f) MLPBC11-DrSh, g) MLPBC10-Steel, h) MLPBC11-Steel, i) MLPBC10-Spread, j) MLPBC11-Spread.

Figure 7. a) MCMC simulation samples, b) cumulative mean, and c) cumulative standard deviation - Problem *11*

Figure 8. CDF of the prior and posterior distributions for dp_{Dr} - Problem*11*

Figure 9. CDF of the prior and marginal posterior distributions for a) dp_{Dr}, b) f_u, and c) q_p - Problem*10*

Figure 10. Joint posterior distribution of a) dp_{Dr} vs. f_u, b) dp_{Dr} vs. q_p, *and c)* f_u vs. q_p - Problem *10*

Figure 11. Prior (a) vs posterior (b) distributions for *FT* - Problem*01*

Figure 12. Joint posterior distributions of a) dp_{Cn} vs. $D_{Cn,}$ b) dp_{Dr} vs. D_{Dr} - Problem *01*

Figure 13. Prior (a) vs posterior (b) distributions for *FT* - Problem*00*

Figure 14. Joint posterior distribution of: a) dp_{Cn} vs. $D_{Cn,}$ b) dp_{Dr} vs. $D_{Dr\,,}$ c) f_u vs. q_p, d) dp_{Dr} vs. q_p, e) dp_{Dr} vs. f_u - Problem *00*

Figure 15. Comparison of $CI_{95\%}$ from the posterior distributions of dp_{Dr} for all problem scenarios

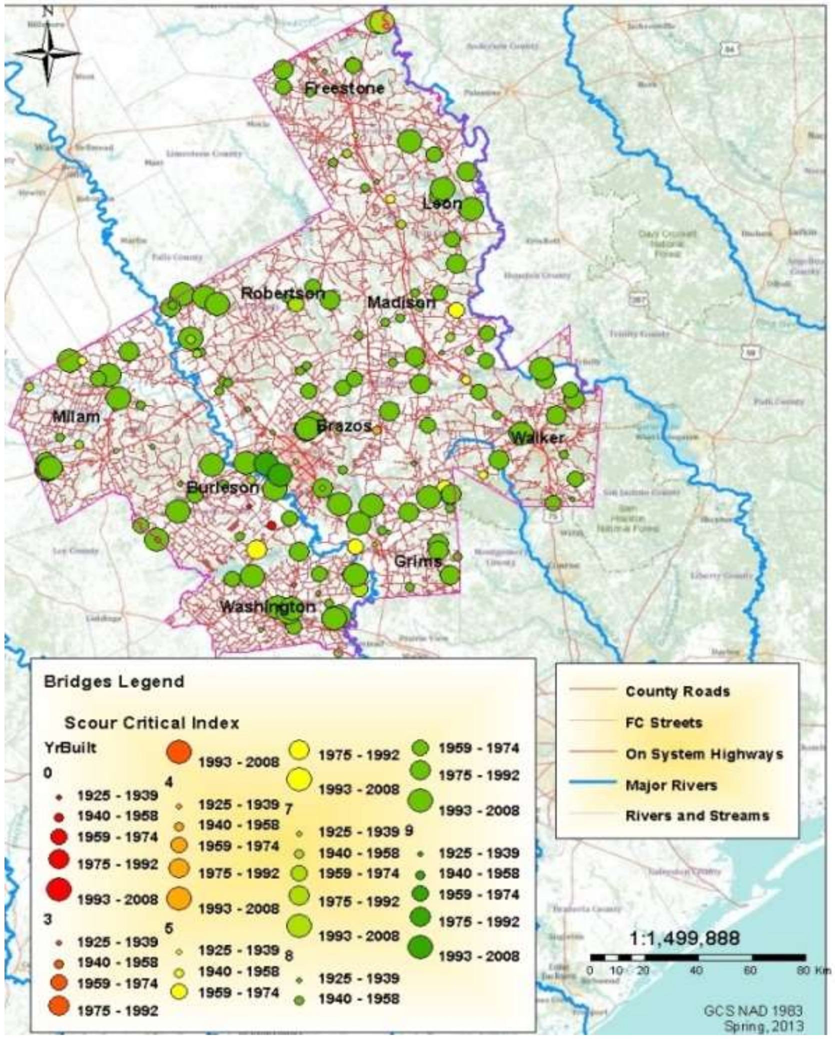

Figure 2. Bridges in the Bryan District of TxDOT included in the working database, showing the Scour-Critical Index and Year Built over the participating counties

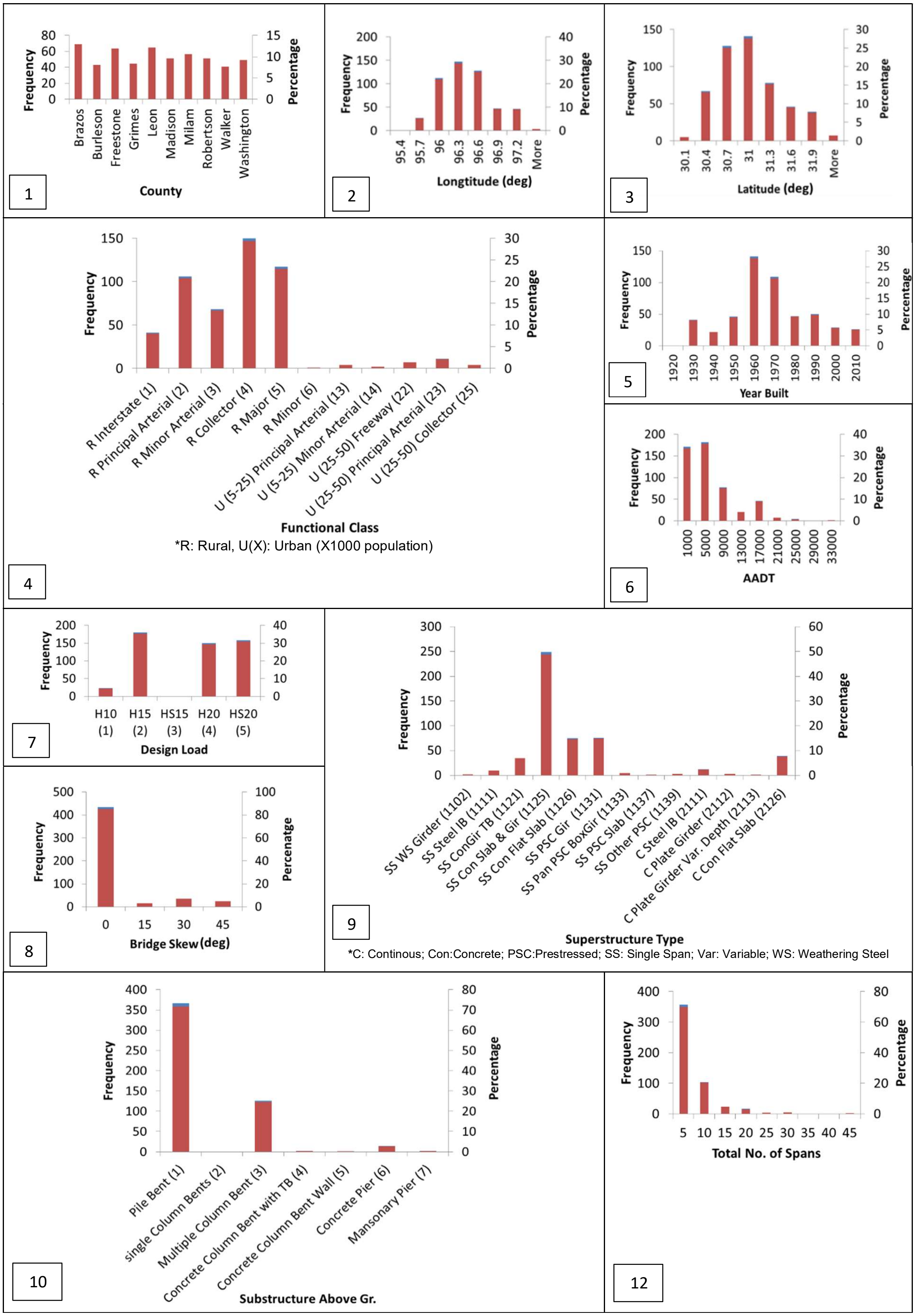

1
Frequency
Percentage
Brazos
Burleson
Freestone
Grimes
Leon
Madison
Milam
Robertson
Walker
Washington
County
2
Frequency
Percentage
95.4
95.7
96
96.3
96.6
96.9
97.2
More
Longtitude (deg)
3
Frequency
Percentage
30.1
30.4
30.7
31
31.3
31.6
31.9
More
Latitude (deg)
4
Frequency
Percentage
R Interstate (1)
R Principal Arterial (2)
R Minor Arterial (3)
R Collector (4)
R Major (5)
R Minor (6)
U (5-25) Principal Arterial (13)
U (5-25) Minor Arterial (14)
U (25-50) Freeway (22)
U (25-50) Principal Arterial (23)
U (25-50) Collector (25)
Functional Class
*R: Rural, U(X): Urban (X1000 population)
5
Frequency
Percentage
1920
1930
1940
1950
1960
1970
1980
1990
2000
2010
Year Built
6
Frequency
Percentage
1000
5000
9000
13000
17000
21000
25000
29000
33000
AADT
7
Frequency
H10 (1)
H15 (2)
HS15 (3)
H20 (4)
HS20 (5)
Design Load
8
Frequency
Percenatge
0
15
30
45
Bridge Skew (deg)
9
Frequency
Percentage
SS WS Girder (1102)
SS Steel IB (1111)
SS ConGir TB (1121)
SS Con Slab & Gir (1125)
SS Con Flat Slab (1126)
SS PSC Gir (1131)
SS Pan PSC BoxGir (1133)
SS PSC Slab (1137)
SS Other PSC (1139)
C Steel IB (2111)
C Plate Girder (2112)
C Plate Girder Var. Depth (2113)
C Con Flat Slab (2126)
Superstructure Type
*C: Continous; Con:Concrete; PSC:Prestressed; SS: Single Span; Var: Variable; WS: Weathering Steel
10
Frequency
Percentage
Pile Bent (1)
single Column Bents (2)
Multiple Column Bent (3)
Concrete Column Bent with TB (4)
Concrete Column Bent Wall (5)
Concrete Pier (6)
Mansonary Pier (7)
Substructure Above Gr.
12
Frequency
Percentage
5
10
15
20
25
30
35
40
45
Total No. of Spans

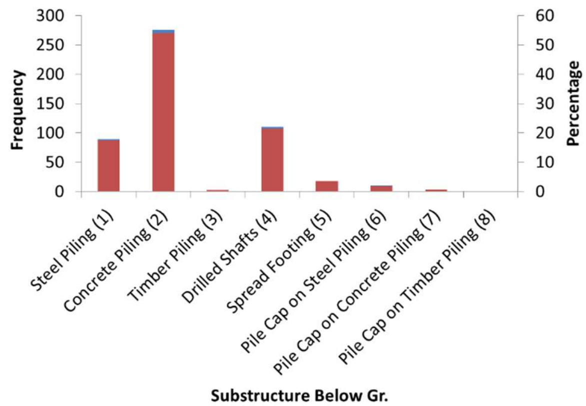

11

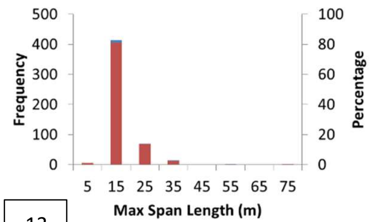

13

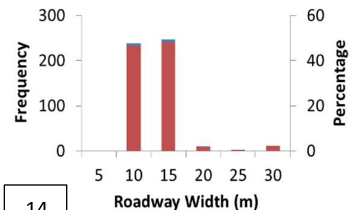

14

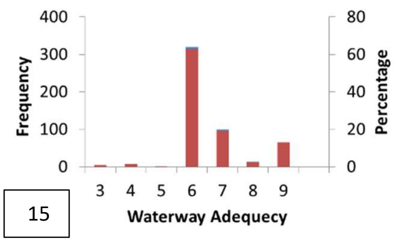

15

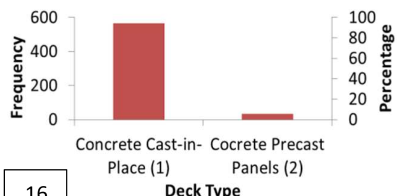

16

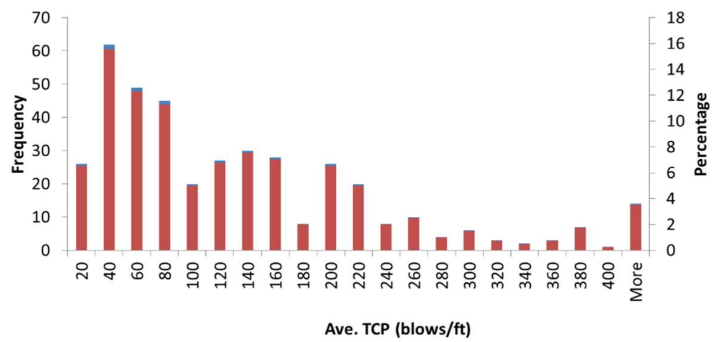

* The equivalent value of TCP for 1ft (30 cm) of penetration was calculated for TCP=100 with less than 1ft penetration.

17

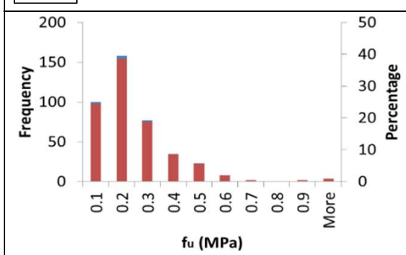

18

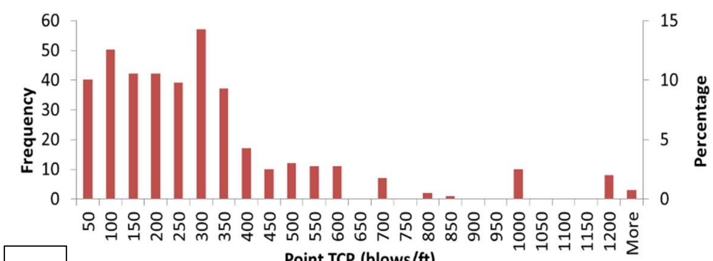

19

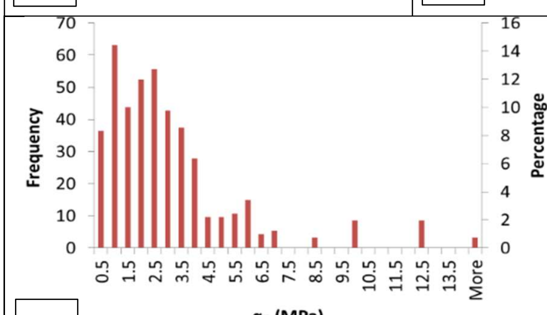

20

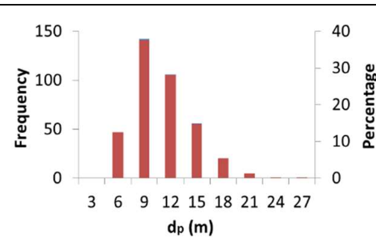

21

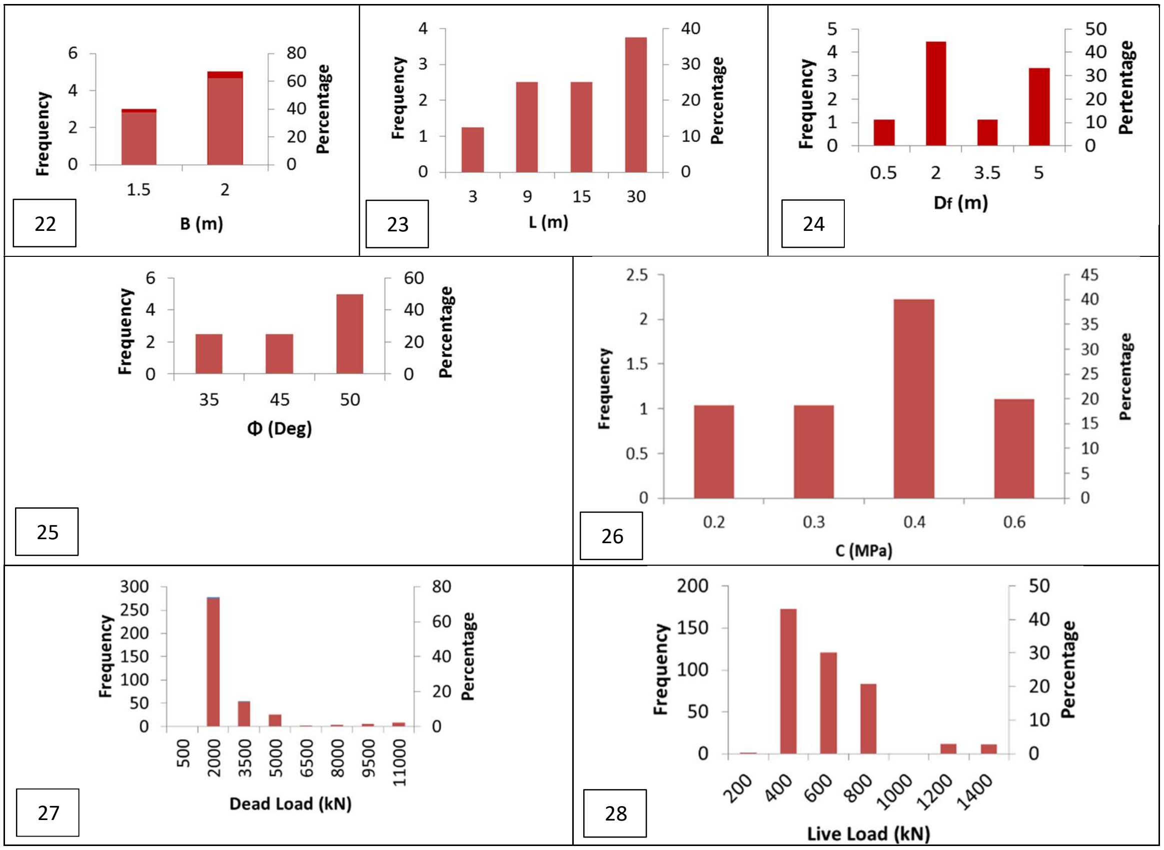

Figure 2. Histograms of database parameters as defined in Table 1

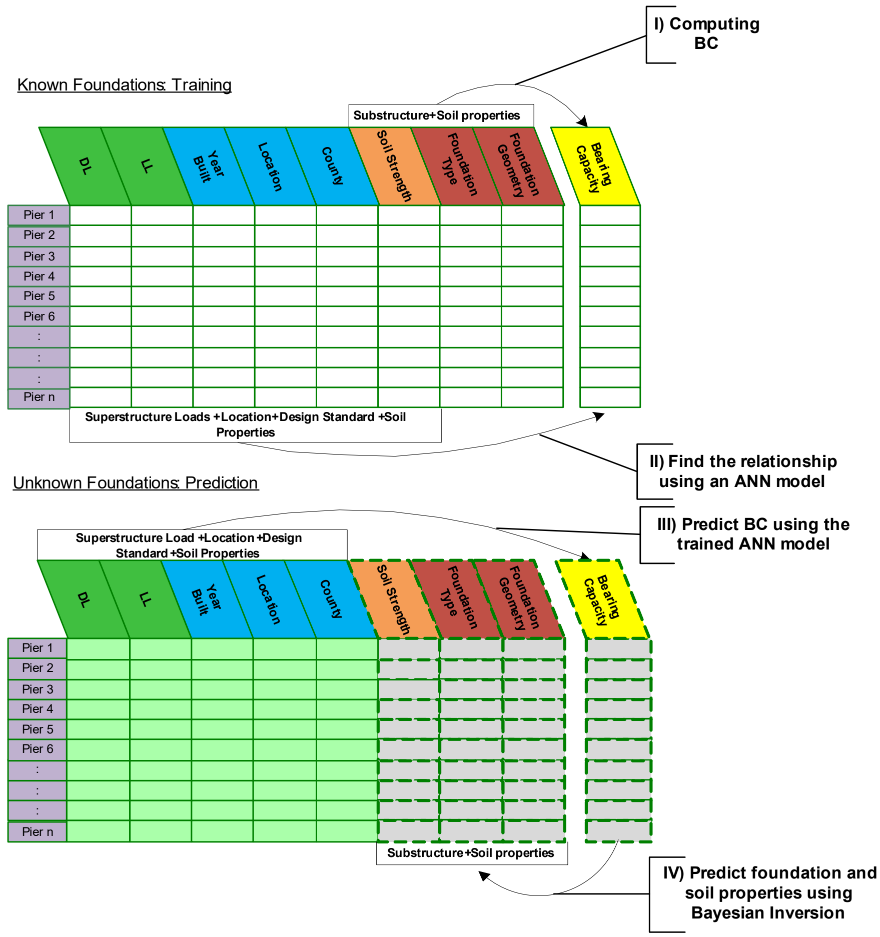

Figure 3. Diagram showing the steps for probabilistic determination of unknown foundations

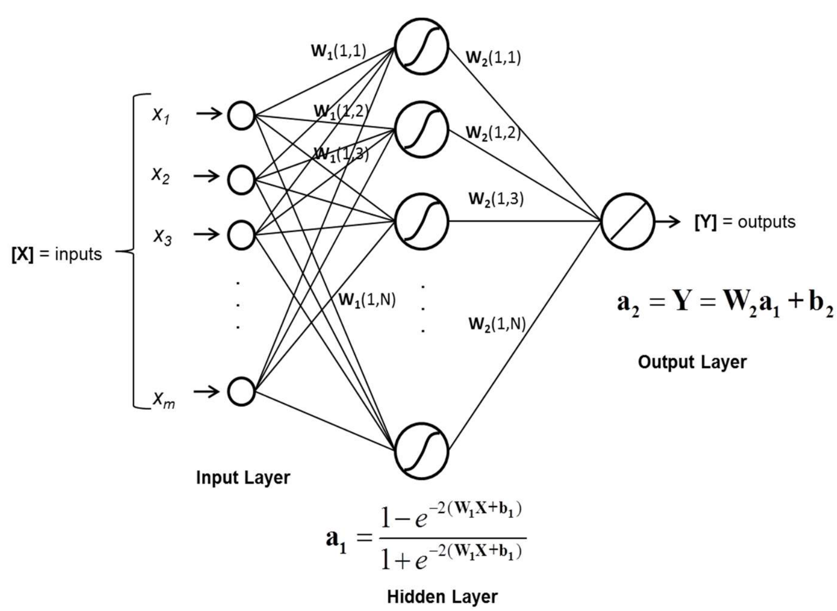

Figure 4. MLP network architecture for BC prediction

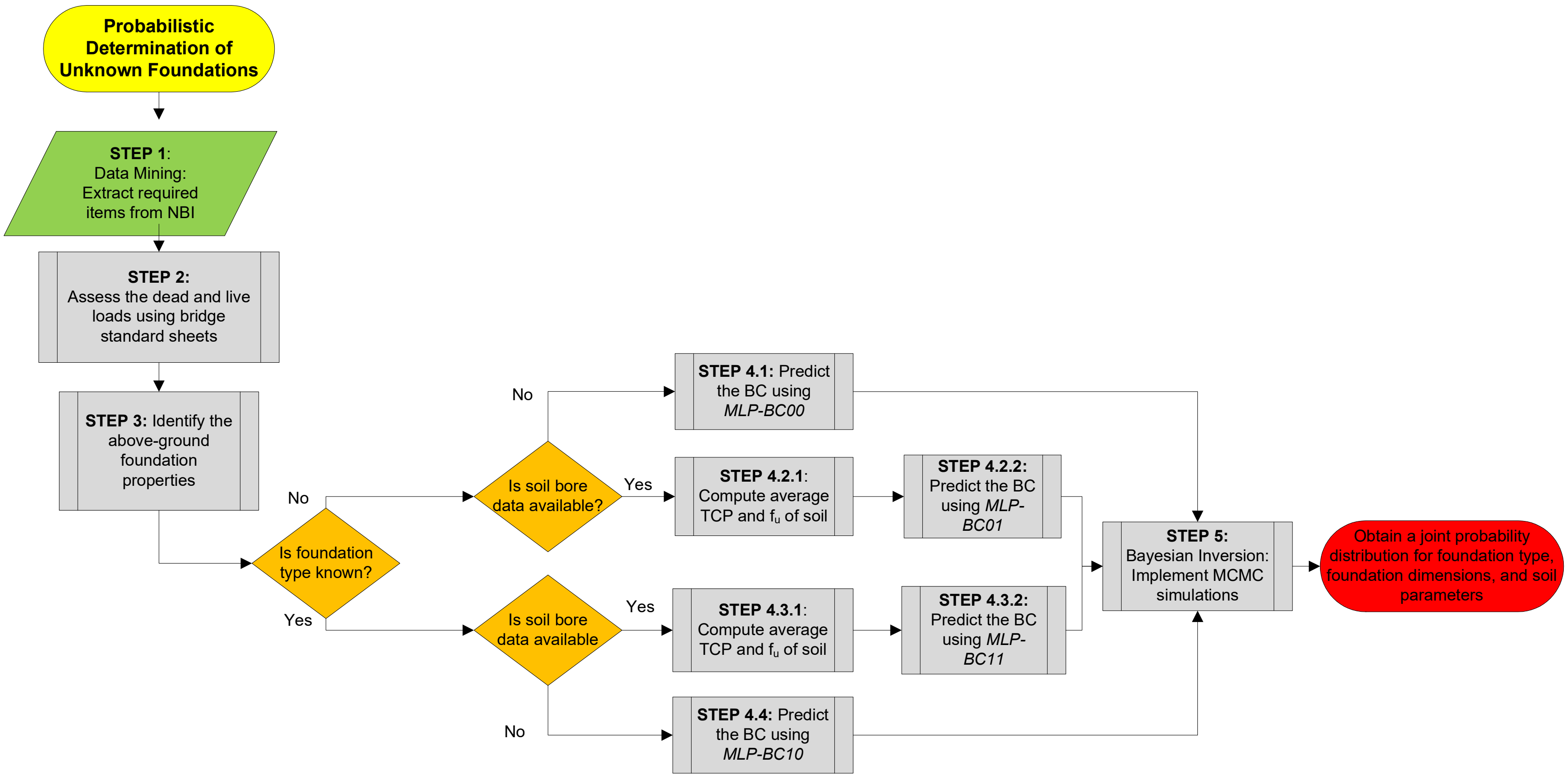

Figure 5. Implementation flowchart of the proposed methodology for probabilistic evaluation of unknown foundations

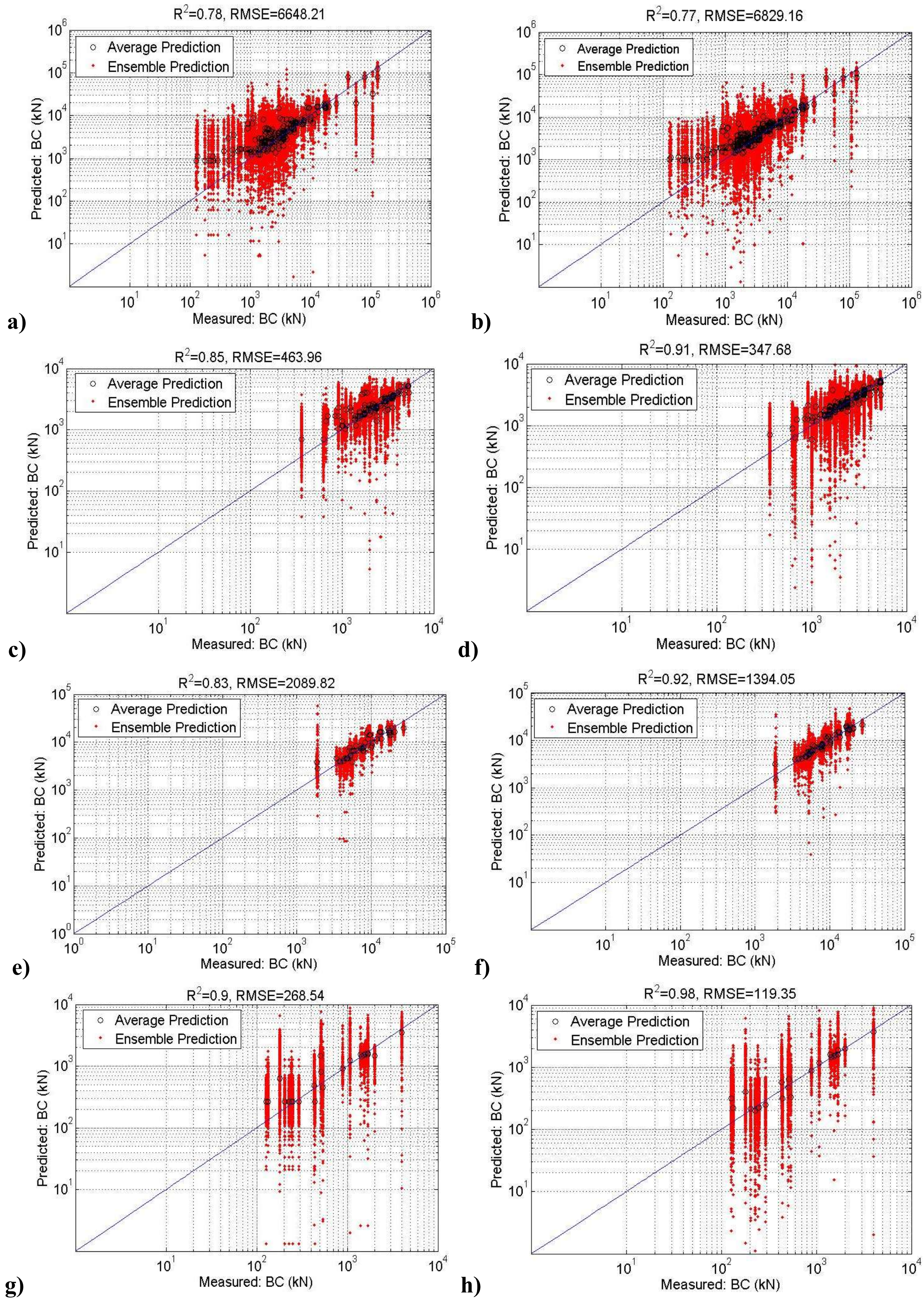

R2=0.78, RMSE=6648.21
R2=0.77, RMSE=6829.16
R2=0.85, RMSE=463.96
R2=0.91, RMSE=347.68
R2=0.83, RMSE=2089.82
R2=0.92, RMSE=1394.05
R2=0.9, RMSE=268.54
R2=0.98, RMSE=119.35
Average Prediction
Ensemble Prediction
Predicted: BC (kN)
Measured: BC (kN)
a)
b)
c)
d)
e)
f)
g)
h)

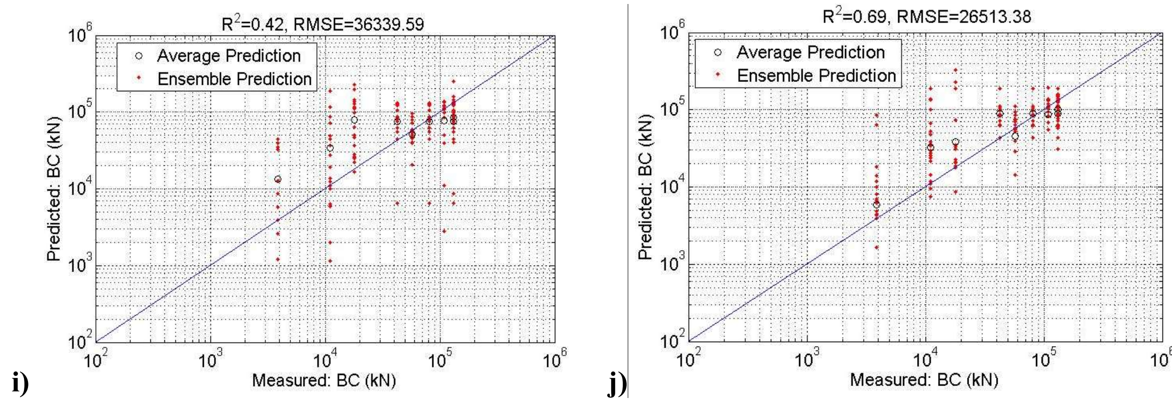

Figure 6. Predictions of BC by MLP ensembles a) MLPBC00, b) MLPBC01, c) MLPBC10-Conc, d) MLPBC11-Conc, e) MLPBC10-DrSh, f) MLPBC11-DrSh, g) MLPBC10-Steel, h) MLPBC11-Steel, i) MLPBC10-Spread, j) MLPBC11-Spread.

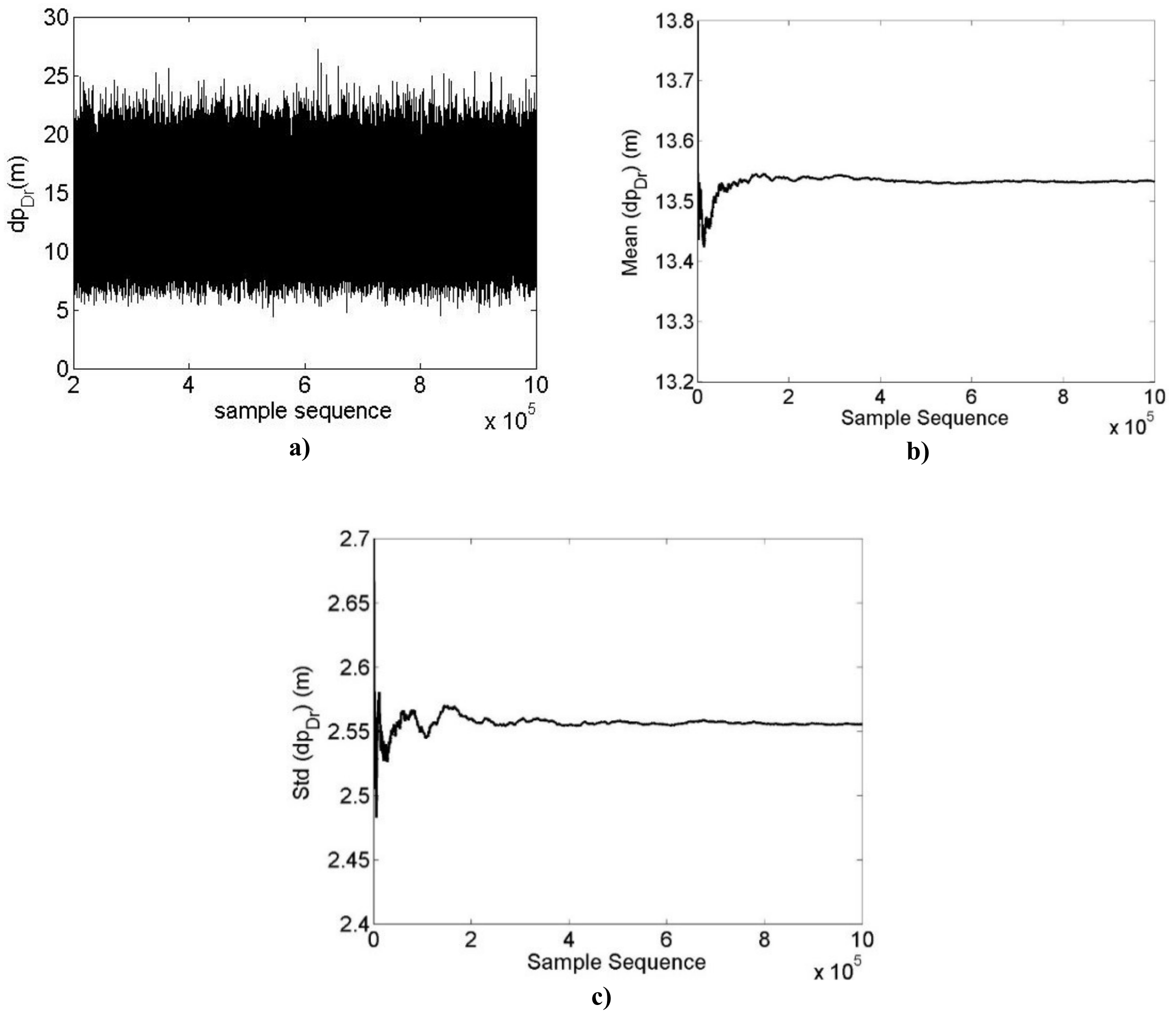

Figure 7. a) MCMC simulation samples, b) cumulative mean, and c) cumulative standard deviation - Problem *11*

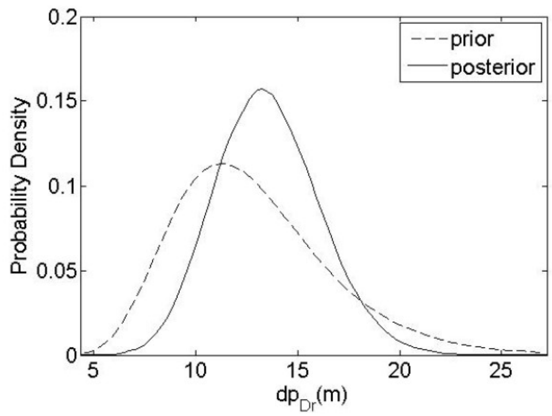

Figure 8. PDF of the prior and posterior distributions for dp_{Dr} - Problem*11*

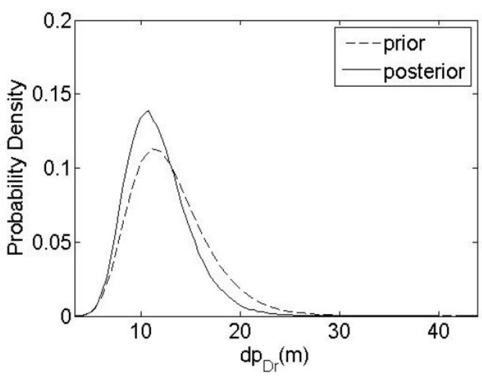

a)

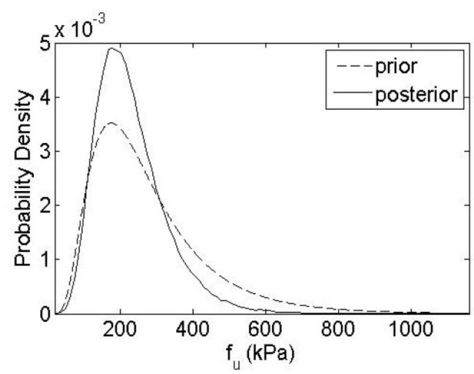

b)

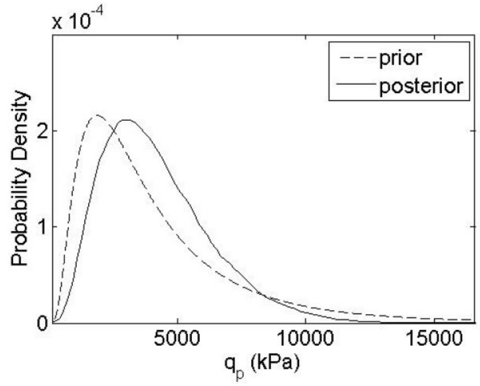

c)

Figure 9. PDF of the prior and marginal posterior distributions for a) dp_{Dr}, b) f_u, and c) q_p - Problem*10*

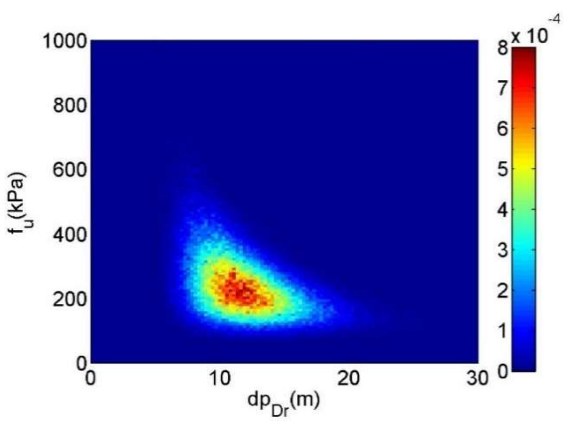

a)

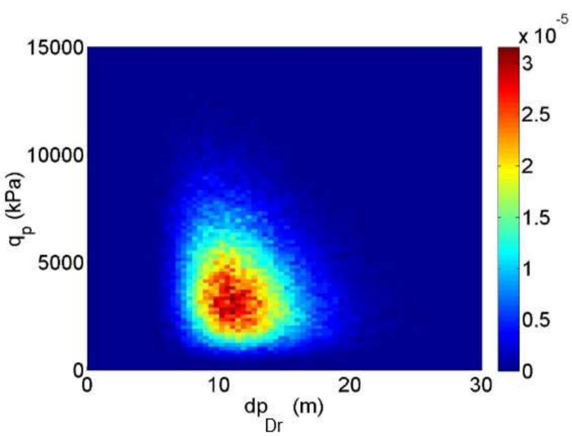

b)

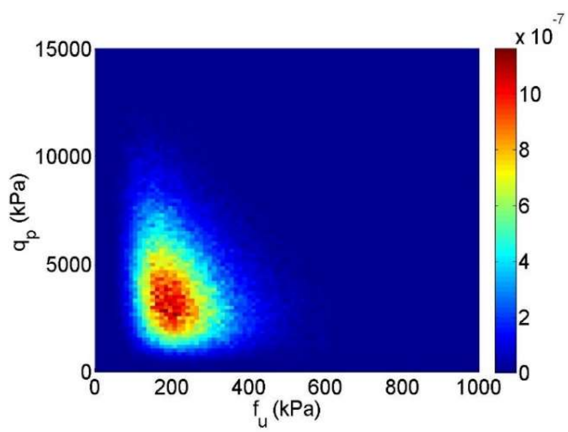

c)

Figure 10. Joint posterior distribution of a) dp_{Dr} vs. f_u, b) dp_{Dr} vs. q_p, *and c)* f_u vs. q_p - Problem *10*

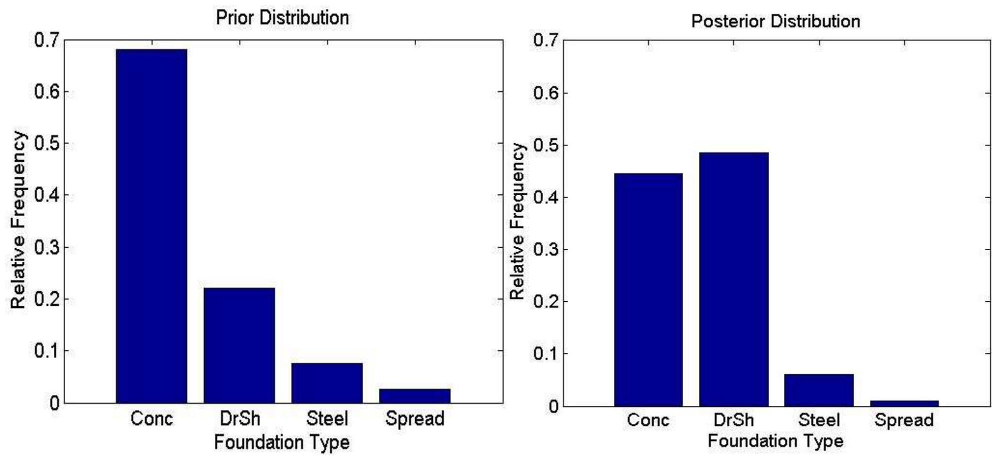

a) b)

Figure 11. Prior (a) vs posterior (b) distributions for *FT* - Problem*01*

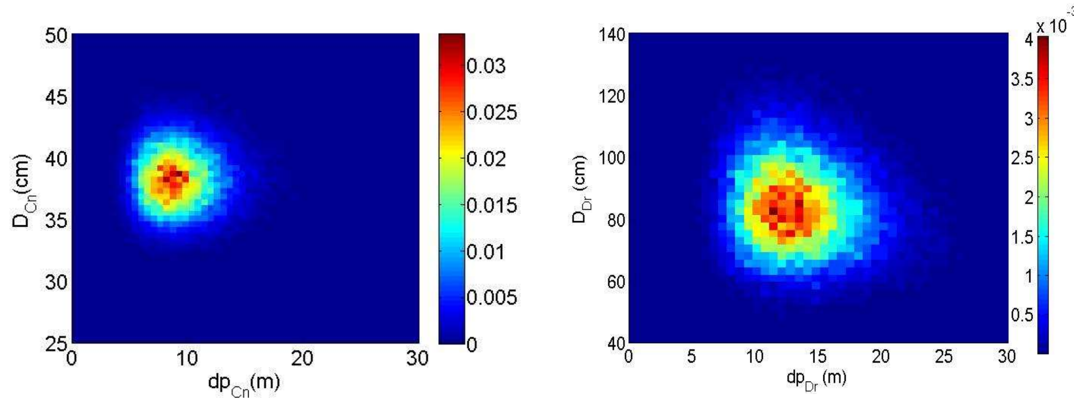

a) b)

Figure 12. Joint posterior distributions of a) dp_{Cn} vs. D_{Cn}, b) dp_{Dr} vs. D_{Dr} - Problem *01*

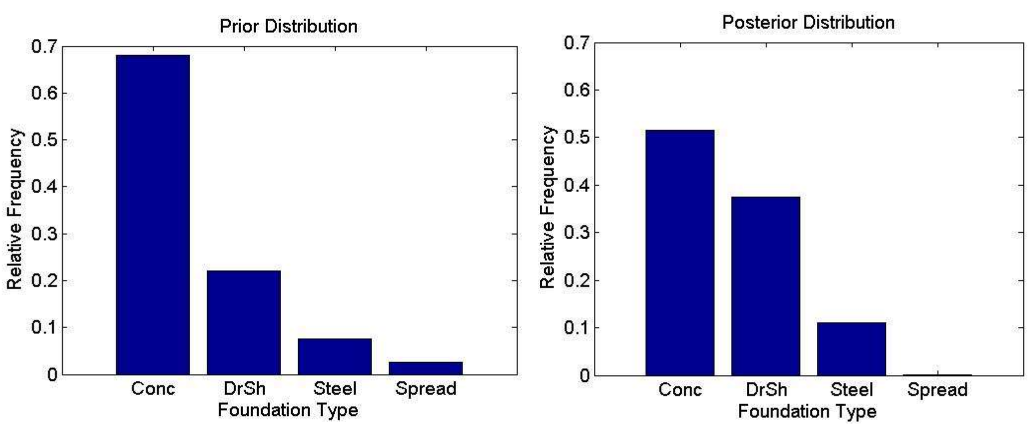

a) b)

Figure 13. Prior (a) vs posterior (b) distributions for *FT* - Problem*00*

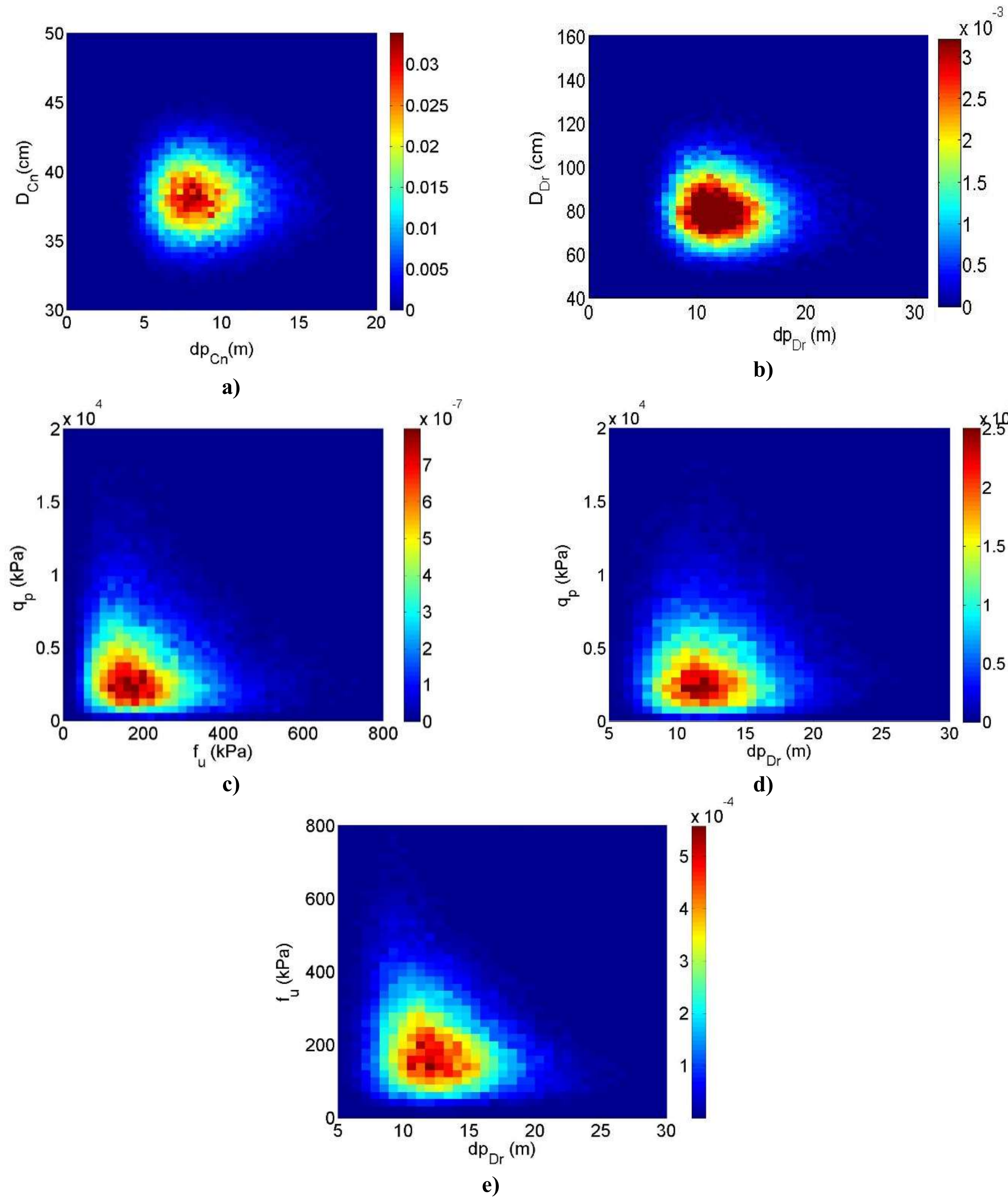

Figure 14. Joint posterior distribution of a) *dp_{Cn}* vs. *D_{Cn}*, b) *dp_{Dr}* vs. *D_{Dr}*, c) *f_u* vs. *q_p*, d) *dp_{Dr}* vs. *q_p*, e) *dp_{Dr}* vs. *f_u* - Problem *00*

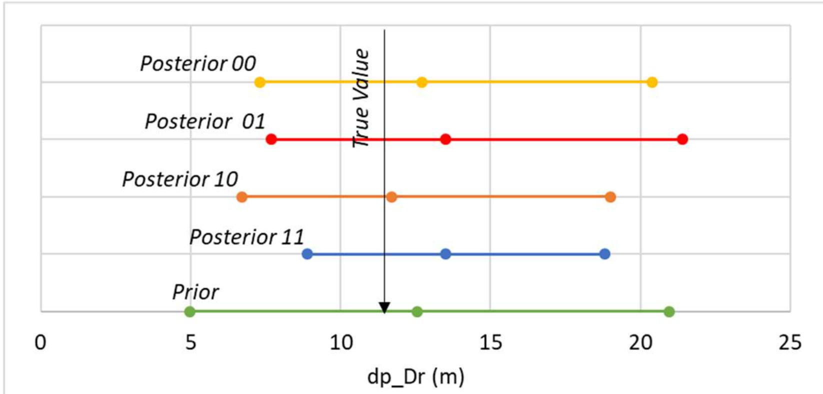

Figure 15. Comparison of $CI_{95\%}$ from the posterior distributions of dp_{Dr} for all problem scenarios